Electronic Supplementary Information

Host-guest recognition coupled with triple signal amplification endows an electrochemiluminescent biosensor with enhanced sensitivity

Min-hui Zhao, Lin Cui*, Chun-yang Zhang*

College of Chemistry, Chemical Engineering and Materials Science, Collaborative Innovation Center of Functionalized Probes for Chemical Imaging in Universities of Shandong, Key Laboratory of Molecular and Nano Probes, Ministry of Education, Shandong Provincial Key Laboratory of Clean Production of Fine Chemicals, Shandong Normal University, Jinan 250014, China

* Corresponding authors. E-mail: cyzhang@sdnu.edu.cn; zpbzcl@126.com; Tel.: +86 0531-86186033. Fax: +86 0531-82615258.

MATERIALS AND METHODS

Materials. Tris(hydroxymethyl)aminomethane (Tris), hydrogen tetrachloroaurate ($HAuCl_4 \cdot 4H_2O$), mercaptohexanol and 2-aminoterephthalic acid luminol were purchased from Sigma-Aldrich Chemical Co. (St. Louis, MO, USA). Potassium hexacyanoferrate (II) trihydrate ($K_4Fe(CN)_6 \cdot 3H_2O$) was obtained from Sinopharm Chemical Reagent Co., Ltd. (Beijing, China). Graphene oxide (GO) was purchased from XFNANO Materials Tech Co., Ltd. (Nanjing, China). Uracil glycosylase inhibitor (UGI), uracil DNA glycosylase (UDG), human alkyladenine DNA Glycosylase (hAAG), 10× UDG reaction buffer (10 mM DTT, 200 mM Tris-HCl, pH 8.0, 10 mM EDTA) were purchased from New England Biolabs Inc. (Beverly, MA, USA). Bovine serum albumin (BSA) was obtained from Sigma-Aldrich Company (St. Louis, MO, USA). The

oligonucleotide was synthesized by Sangon Biological Engineering Technology & Services Co., Ltd. (Shanghai, China). The hairpin DNA sequences is 5'-HS-*UUU GUC UGU GA*A GGA GGT AGA *TCA CAG ACA AA*-$(CH_2)_6$-Fc-3' (the cutting bases are shown with underline, and the binding regions are shown with italic). Human cervical carcinoma cell line (HeLa cells) was purchased from Cell Bank, Shanghai Institutes for Biological Sciences (Shanghai, China).

Apparatus and Characterization. Electrochemiluminescence signals were obtained by a MPI-EII multifunctional electrochemical and chemiluminescent analytical system (Xi'an Remex Analytical Instrument Co., Ltd., China), in which the emission window lays above the photomultiplier tube biased at 600 V. Electrochemiluminescent measurements were performed with three-electrode system including a modified glassy carbon electrode (GCE, 4 mm in diameter), a platinum wire, and a Ag/AgCl (saturated KCl). Electrochemical impedance spectroscopy (EIS) was obtained by a Zahner workstation (Zahner, German). Scanning electron microscopic (SEM) images were obtained by a SU-8010 (Hitachi) scanning electronic microscope (Hitachi, Japan). Powder X-ray diffraction (XRD) patterns were measured by a Rigaku D/MAX 2200PC X-ray diffractometer (X'Pert Pro Super, Philips). The transmission electron micrographs (TEM) were obtained by a JEOL JEM 2010 electron microscope (JEOL Ltd., Japan). The ESP-300E spectrometer (Bruker, Germany) was used for recording electron spin resonance (EPR) spectra at room temperature. Zeta potential was measured by using a Malvern zeta sizer Nano-ZS90 (Malvin Inst. Co. Ltd. England). Absorption spectra were obtained by a pharmaspec UV-3900 UV-visible spectrophotometer (Hitachi, Japan).

Synthesis of FeMOF and the AuNPs@luminol. FeMOF was synthesized based on the reported method.[1] The 0.187 g of $FeCl_3 \cdot 6H_2O$ and 0.126 g of 2-aminoterephthalic acid were mixed in

dimethyl formamide (DMF, 15 mL), followed by the addition of acetic acid (3.45 mmol) and incubation for 4 h at 120 ^{o}C in an oil bath for crystallization. When the reaction solution was cooled to room temperature, the particles were centrifuged at 4000 rpm for isolation, and the excess reactants were removed by washing with ethanol and DMF. The obtained particles were dried in a vacuum oven.

The AuNPs@luminol nanohybrids were synthesized by the reduction of $HAuCl_4$ with luminol according to the reported method.[2] All glassware used in this experiment was cleaned in freshly prepared aqua regia (HNO_3 /HCl = 1:3, v/v), followed by washing with double-distilled deionized water and drying. The 100 mL of 0.01 wt% $HAuCl_4$ solution was heated to boiling point, followed by rapid addition of 1.6 mL of 0.01 M luminol with stirring vigorously for 30 min. The solution turned to wine-red from yellow. Then the heating source was removed, and the colloids were cooled to room temperature for another 20 min prior to storing at 4 °C.

Preparation of the FeMOF/AuNPs@luminol-Hairpin Probe. The modification of FeMOF with the AuNPs@luminol was achieved by mixing 2 mL of 1 mg mL^{-1} FeMOF with 4 mL of AuNPs@luminol and shaking vigorously for 2 h. Then the FeMOF/AuNPs@luminol composites were centrifuged at 5000 rpm, followed by dispersion in 1 mL of 10 mM Tris-HCl (pH 7.4). The 10 μM hairpin probes were denatured in 1.5 mM $MgCl_2$ and 10 mM Tris-HCl (pH 8.0) at 95 °C for 5 min, and then cooled to room temperature to form the hairpin structure. The FeMOF/AuNPs@luminol-hairpin probes were obtained by incubating the FeMOF/AuNPs@luminol with 200 μL of 10 μM hairpin probes for 12 h at 4 °C, followed by centrifugation at 5000 rpm.

Fabrication of Electrochemiluminescent Platform. The GC electrode with a mirror-like surface

was obtained by polishing with 1.0, 0.3 and 0.05 μm α-Al_2O_3 slurries and subsequently sonicating with ethanol and water. The *β*-CD/GO/GCE was obtained by sequentially dropping 20 μL of GO (0.25 mg mL^{-1}) and 20 μL of 2 mM *β*-CD on the GC electrode, followed by evaporating solvent, rinsing with water, and drying in air.

Detection of UDG and Inhibition Assay. The FeMOF/AuNPs@luminol-hairpin probes (10 μL) were mixed with 10× UDG reaction buffer (2 μL) and different-concentration UDG in a total volume of 20 μL, followed by incubation with the *β*-CD/GO/GCE for 80 min at 37 °C and then transferring the electrode to the solution (10 mM HCl and 0.5 mM $K_4Fe(CN)_6$) for another 45-min incubation to form prussian blue on the surface of electrode. The ECL measurements were performed in PBS solution (pH 10.0) containing 5 mM H_2O_2.[3,4] UDG inhibition assay was performed using similar procedures except for the pre-incubation of inhibitors with 1 U mL^{-1} UDG in reaction solution.

Cell Culture. HeLa cells were grown in Dulbecco's modified Eagle's medium supplemented with 1% penicillin-streptomycin and 10% fetal bovine serum at 37 °C with 5% CO_2. The cells were harvested by using trypsinization and suspended in the lysis buffer (150 mM NaCl, 10 mM Tris-HCl, pH 8.0, 0.25 mM sodium deoxycholate, 1% NP-40, 0.1 mM 4-(2-aminoethyl) benzenesulfonyl fluoride hydrochloride, and 1.0% glycerol,), followed by incubation for 30 min on ice and centrifugation for 20 min at 12000 g at 4 °C. The obtained supernatant was stored at −80 °C.

SUPPLEMENTARY RESULTS

The OH• radical can be identified by 5,5-dimethyl-1-pyrroline N-oxide (DMPO). The 1:2:2:1 quartet characteristic peak of typical DMPO−OH• adduct is observed when DMPO is introduced into the luminol–prussian blue–H_2O_2 system (Fig. S1), indicating the involvement of OH• in CL emission process.

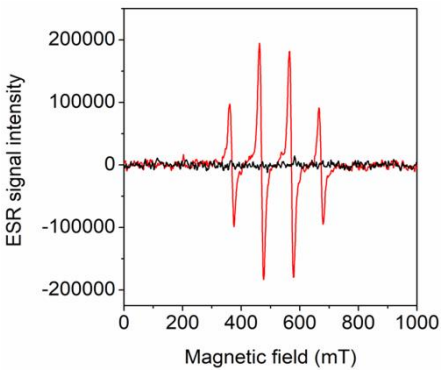

Fig. S1 EPR spectra of $OH^{\bullet}$ radicals in luminol–H_2O_2 (black line) and luminol–prussian blue–H_2O_2 (red line) systems.

Assay Feasibility. The electrochemical impedance spectra (EIS) were used for interfacial study. Fig. S2A shows the EIS of modified electrodes in different construction steps and the corresponding equivalent circuit (inset of Fig. S2A). The bare GCE displays a charge-transfer resistance (R_{ct}) of 502 Ω, indicating the diffusion of $Fe(CN)_6^{3-/4-}$ to the electrode surface (Fig. S2A, curve a). The GO-modified GCE (Fig. S2A, curve b) exhibits a high R_{ct} of 1600 Ω compared with the bare electrode. This can be explained by the fact that the less conductive and negatively charged GO can repel the negatively charged redox probe $Fe(CN)_6^{3-/4-}$. The dropping of β-CD on the GO-modified GCE results in a R_{ct} of 2734 Ω (Fig. S2A, curve c) due to the introduction of non-conductive β-CD. When the β-CD/GO/GCE is incubated with 1 U mL^{-1} UDG and the FeMOF/AuNPs@luminol-hairpin probes for 80 min, a R_{ct} of 5917 Ω is observed (Fig. S2A, curve

d) as a result of the steric hindrance of FeMOF and the electrostatic repulsion effect between DNA and $Fe(CN)_6^{3-/4-}$.

We further investigated the β-CD/GO/GCE with different modified surfaces (Fig. S2B). When the β-CD/GO/GCE is incubated with the FeMOF/AuNPs@luminol-hairpin probes and UDG, a high ECL signal is observed (Fig. S2B, curve c) compared with that in the absence of UDG (Fig. S2B, curve a). When 1 U mL^{-1} UDG is present, the ECL signal of the FeMOF/AuNPs@luminol-hairpin probe + formation of prussian blue (Fig. S2B, curve d) has been enhanced by 8- and 3-fold compared with that of the AuNPs@luminol-hairpin probe (Fig. S2B, curve b) and the FeMOF/AuNPs@luminol-hairpin probe (Fig. S2B, curve c), respectively, indicating that the introduction of prussian blue and Fc on the electrode can catalyze the deposition of H_2O_2 to produce $OH^{\bullet}$ for the generation of an enhanced ECL signal in the luminol–H_2O_2 system.

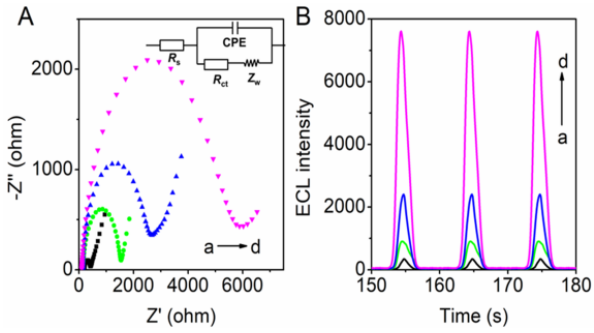

Fig. S2 (A) EIS characterization of the modified GCE electrodes: (a) GCE, (b) GO/GCE, (c) *β*-CD/GO/GCE, and (d) *β*-CD/GO/GCE incubating with the FeMOF/AuNPs@luminol-hairpin probes and 1 U mL^{-1} UDG. Inset shows electrical equivalent circuit for impedance data fitting. Z_w, Warburg impedance; R_s, Ohmic resistance; CPE, constant phase angle element; R_{ct}, charge-transfer resistance. (B) ECL signal of the *β*-CD/GO/GCE in response to the FeMOF/AuNPs@luminol-hairpin probes (a), the AuNPs@luminol-hairpin probes + 1 U mL^{-1}

UDG (b), the FeMOF/AuNPs@luminol-hairpin probes + 1 U mL^{-1} UDG (c), the FeMOF/AuNPs@luminol-hairpin probes + 1 U mL^{-1} UDG + the formation of prussian blue (d).

Optimization of Experimental Parameters. To obtain high assay performance, we optimized following experimental parameters: the concentrations of *β*-CD, $Fe(CN)_6^{4-}$ and FeMOF/AuNPs@luminol hairpin probes, reaction time of FeMOF with $Fe(CN)_6^{4-}$ for the formation of prussian blue, reaction time of the FeMOF/AuNPs@luminol-hairpin probes with UDG (Fig. S3). Fig. S3A shows the influence of *β*-CD concentration upon the ECL signal. With the increase of the *β*-CD concentration from 1 to 5 mM, ECL signal enhances greatly and reaches a maximum value at the concentration of 2 mM. The higher the *β*-CD concentration, the more the FeMOF/AuNPs@luminol-hairpin probes being captured on the *β*-CD/GO/GCE. Thus, the optimized concentration of *β*-CD is 2 mM. The concentration of $Fe(CN)_6^{4-}$ plays an important role in the formation of prussian blue. As shown in Fig. S3B, the ECL signal enhances with the increasing concentration of $Fe(CN)_6^{4-}$ in the range of 0.1– 0.5 mM. When the concentration of $Fe(CN)_6^{4-}$ is more than 0.5 mM, the ECL signal decreases dramatically. The signal-to-noise (S/N) ratio (refers to the ratio of ECL intensity in the presence of UDG to the ECL intensity in the absence of UDG) reaches a maximum value at the concentration of 0.5 mM. Thus, 0.5 mM $Fe(CN)_6^{4-}$ is used in the subsequent research. The concentration of the FeMOF/AuNPs@luminol hairpin probes was optimized as well (Fig. S3C). The ECL signal enhances with the increasing concentration of the FeMOF/AuNPs@luminol-hairpin probes from 0.4 to 1 μM. When the concentration of the FeMOF/AuNPs@luminol-hairpin probes is more than 1 μM, the ECL signal levels off. Thus, 1 μM FeMOF/AuNPs@luminol-hairpin probe is used in the subsequent research.

In addition, ECL signal enhances with the reaction time of the FeMOF/AuNPs@luminol-hairpin probes with UDG from 40 to 120 min, and reaches a maximum value at 80 min (Fig. S3D). We further optimized the reaction time of FeMOF with $Fe(CN)_6^{4-}$ for the formation of prussian blue. As shown in Fig. S3E, ECL signal enhances rapidly with the incubation time of $Fe(CN)_6^{4-}$ with the FeMOF/AuNPs@luminol-hairpin probe from 20 to 50 min, and levels off beyond 50 min. The S/N ratio reaches a maximum value at 50 min. Therefore, reaction time of 50 min is used for the formation of prussian blue in the subsequent research.

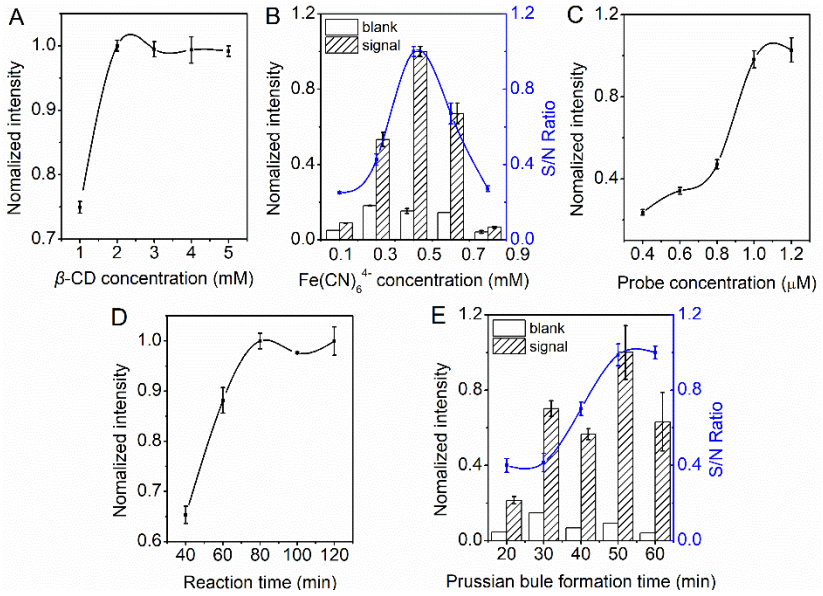

Fig. S3 Effect of (A) β-CD concentration, (B) $Fe(CN)_6^{4-}$ concentration, (C) the FeMOF/AuNPs@luminol-hairpin probe concentration, (D) reaction time of the FeMOF/AuNPs@luminol-hairpin probe with 1 U mL^{-1} UDG, and (E) reaction time of the FeMOF/AuNPs@luminol-hairpin probe with $Fe(CN)_6^{4-}$ for the formation of prussian blue. Error bars show standard derivation obtained from three independent experiments.

UDG Inhibition Assay. We used UGI as a model inhibitor to demonstrate the application of this ECL biosensor for inhibition assay. UGI can form a tight and physiologically irreversible complex

with UDG in 1:1 M stoichiometry.[5] The relative activity (RA) of UDG is calculated according to eq. 1:

$$\text{RA}\ (\%) = \frac{N_i - N_0}{N_t - N_0} \times 100\% \qquad (1)$$

where N_o represents the ECL intensity without UDG, N_t represents the ECL intensity when 1 U mL^{-1} UDG is present, and N_i represents the ECL intensity when 1 U mL^{-1} UDG and 1 U mL^{-1} UGI are present. Fig. S4 shows that UGI can induce the decrease of UDG relative activity in a concentration-dependent manner. An IC_{50} value (the UGI concentration for 50% inhibition of UDG activity) of 0.6464 U mL^{-1} is obtained, consistent with the previous research,[6] suggesting the feasibility of this ECL biosensor for screening UDG inhibitors.

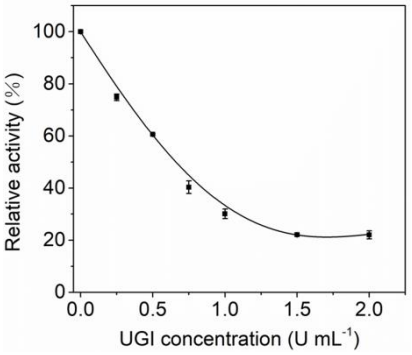

Fig. S4 Variance of relative activity of UDG (1 U mL^{-1}) with the increasing concentration of UGI. Error bars are standard derivation obtained from three independent experiments.

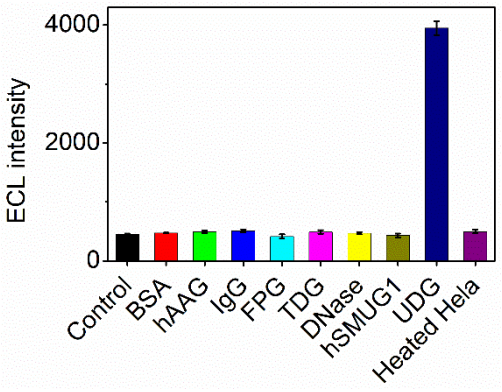

Fig. S5 Measurement of the ECL signal in response to the control group without cell extracts, 0.01 mg mL^{-1} BSA, 1 U mL^{-1} hAAG, 0.01 mg mL^{-1} IgG, 1 U mL^{-1} FPG, 1 U mL^{-1} TDG, 1 U mL^{-1} DNase, and 1 U mL^{-1} hSMUG1, cell lysate corresponding to 10000 Hela cells (UDG), and the

heated Hela cell lysate (Heated Hela), respectively. Error bars show standard derivation obtained from three independent experiments.

Table S1. Comparison of the proposed ECL biosensor with reported methods for UDG assay

Detection methods	Linear range (U mL^{-1})	Detection limit (U mL^{-1})	Refs.
electrochemiluminescence	0.0005 - 1	2.5×10^{-4}	this work
electrochemiluminescence	0.02 - 22	0.006	7
electrochemistry	0.025 - 2	0.012	8
electrochemistry	0.05 - 1.1	0.01	9
electrochemistry	0.01 - 10	0.0079	10
fluorescence	0.0008 - 0.1	0.0008	11
fluorescence	0.002 - 1.0	0.002	12
fluorescence	0.005 - 5	0.0025	13
colorimetry	0.06 - 8	0.02	14

Table S2. Recovery studies in human serum samples.

Added (U mL^{-1})	Measured (U mL^{-1})	Recovery (%)	RSD (%)
0.01	0.0098	98.0	1.5
0. 1	0.102	102.0	3.2
1	0.97	97.0	3.5

References

1. Liu, Y. L.; Zhao, X. J.; Yang, X. X.; Li, Y. F. *Analyst* 2013, **138**, 4526-4531.
2. Surblé, S.; Serre, C.; Mellot-Draznieks, C.; Millange, F.; Férey, G. *Chem. Commun.* 2006, 284-286.
3. He, Y.; He, X.; Liu, X.; Gao, L.; Cui, H. *Anal. Chem.* 2014, **86**, 12166-12171.
4. Wang, S.; Zhao, Y.; Wang, M.; Li, H.; Saqib, M.; Ge, C.; Jin, Y. *Anal. Chem*, 2019, **91**, 3048-3054.
5. Kaushal, P. S.; Talawar, R. K.; Krishna, P.; Varshney, U.; Vijayan, M. *Acta Crystallogr., Sect. D: Biol. Crystallogr.* 2008, **64**, 551-560.
6. Wu, Y.; Wang, L.; Zhu, J.; Jiang, W. *Biosens. Bioelectron.* 2015, **68**, 654-659.
7. Liu, Q.; Liu, C.; Zhu, G.; Xu, H.; Zhang, X. J.; Hu, C.; Xie, Y.; Zhang, K.; Wang, H. *Microchim. Acta.* 2019, **186**, 179.
8. Liu, X.; Chen, M.; Hou, T.; Wang, X.; Liu, S.; Feng, L. *Electrochim. Acta* 2013, **113**, 514-518.
9. Jiao, F.; Qian, P.; Qin, Y.; Xia, Y.; Deng, C.; Nie, Z. *Talanta* 2016, **147**, 98-102.
10. Zhang, H.; Zhang, L.; Jiang, J.; Yu, R. *Anal. Sci*. 2013, **29**, 193-198.
11. Jing, T.; Panshu, S.; Yusuke, S.; Seiichi, N.; Norio, T.; Aijun, T.; Yu, X. *Chem. Commun.* 2014, **51**, 929-932.
12. Zhang, L.; Zhao, J.; Jiang, J.; Yu, R. *Chem. Commun*. 2012, **48**, 8820-8822.
13. Zhang, Y.; Li, C. C.; Tang, B.; Zhang, C. Y. *Anal. Chem.* 2017, 89, 7684-7692
14. Liu, X.; Chen, M.; Hou, T.; Wang, X.; Liu, S.; Feng, L. I. *Biosens. Bioelectron*. 2014, **54**, 598-602.